Data-driven predictive models of diffuse low-grade gliomas under chemotherapy

Meriem Ben Abdallah, Marie Blonski, Sophie Wantz-Mézières, Yann Gaudeau, Luc Taillandier, Jean-Marie Moureaux, Amelie Darlix, Nicolas Menjot de Champfleur, Hugues Duffau

This article has been accepted for publication in a future issue of this journal, but has not been fully edited. Content may change prior to final publication. Citation information: DOI 10.1109/JBHI.2018.2834159, IEEE Journal of Biomedical and Health Informatics

Data-driven predictive models of diffuse low-grade gliomas under chemotherapy

M. Ben Abdallah, M. Blonski, S. Wantz-Mézières, Y. Gaudeau, L. Taillandier, J.-M. Moureaux , A. Darlix, N. Menjot de Champfleur and H. Duffau

***Abstract*—Diffuse Low-Grade Gliomas (DLGG) are brain tumors of young adults. They affect the quality of life of the inflicted patients and, if untreated, they evolve into higher grade tumors where the patient's life is at risk. Therapeutic management of DLGGs includes chemotherapy, and tumor diameter is particularly important for the follow-up of DLGG evolution. In fact, the main clinical basis for deciding whether to continue chemotherapy is tumor diameter growth rate. In order to reliably assist the doctors in selecting the most appropriate time to stop treatment, we propose a novel clinical decision support system. Based on two mathematical models, one linear and one exponential, we are able to predict the evolution of tumor diameter under Temozolomide chemotherapy as a first treatment and thus offer a prognosis on when to end it. We present the results of an implementation of these models on a database of 42 patients from Nancy and Montpellier University Hospitals. In this database, 38 patients followed the linear model and four patients followed the exponential model. From a training dataset of a minimal size of five, we are able to predict the next tumor diameter with high accuracy. Thanks to the corresponding prediction interval, it is possible to check if the new observation corresponds to the predicted diameter. If the observed diameter is within the prediction interval, the clinician is notified that the trend is within a normal range. Otherwise, the practitioner is alerted of a significant change in tumor diameter.**

***Index Terms*—Brain tumor, Chemotherapy, Glioma, MRI, Predictive model, Temozolomide, TMZ.**

I. Introduction

DIFFUSE Low-Grade Gliomas (DLGG) are brain tumors of young adults. If untreated, they inevitably evolve into high-grade gliomas where the functional and then vital prognosis is more severe [1], [2]. The survival rate after five years being between 58% and 72%, this tumor cannot be considered as benign [1].

On the molecular level, data on the presence of an IDH1 mutation and of a 1p/19q co-deletion were integrated into the 2016 WHO classification of gliomas and both are considered as prognostic and/or predictive factors which must now be included in the diagnosis [3]. In more than two-thirds of DLGG cases, 1p/19q co-deletion is directly associated with lower evolution [4], better survival [5] and increased chemosensitivity [4]. On the other hand, 1p/19q non co-deletion is a poor prognostic factor [6]. As for IDH1 mutations, they appear to be typical of DLGGs. In addition, they are associated with a more favorable prognosis, increased chemosensitivity and better overall survival [7].

The management of DLGGs relies on FLAIR or T2 transverse MRI scans [1]. From these MRI sequences, tumor volume V is obtained either through the three diameters method [8] or through a segmentation followed by a software reconstruction method [9]. As previous work by Mandonnet *et al.* [10] demonstrated that tumor diameter is a good predictor of the evolution of DLGGs, a longitudinal follow-up of tumor diameter D is used to monitor DLGG patients. Considering a sphere with a volume equivalent to tumor volume, tumor diameter is calculated as follows:

$$D = (2 \times V)^{1/3}. \tag{1}$$

Based on the estimated tumor diameters obtained from two successive MRIs that are at least three months apart, doctors compute the slope of tumor progression. This slope provides information on the kinetics of tumor progression and allows the detection of rapidly growing gliomas (growth rate $>$ 8 mm/year), a behaviour that is characteristic of high-grade gliomas [1], [8], [11], [12].

The recommended therapeutic options for the treatment of DLGGs include surgery, chemotherapy and radiotherapy. It should be noted that none of these treatments are intended to cure the disease, but rather to limit its evolution and its infiltration in order to extend the survival of the patient while preserving the quality of life as best as possible [13]. Our contribution lies within this framework, as we propose new mathematical models for DLGG progression. Moreover, previous related works and their shortcomings will be discussed in more detail below.

Among the proposed treatments, surgery is the first to be considered for DLGGs because of its positive impact on survival. Indeed, it has been shown that surgery, so long as it excises as much of the lesion as possible, delays the transformation of DLGGs into higher grade gliomas [2]. Patients may be inoperable at the time of diagnosis for various reasons: large tumor infiltration in eloquent areas, a too voluminous glioma, gliomatosis (tumor present throughout the brain) or multifocal

M. Ben Abdallah was with the Université de Lorraine, CRAN, Vandoeuvre-lès-Nancy, France. She is now with the ÉTS, LIO, CRCHUM, Montréal, Canada.

M. Blonski and L. Taillandier are with the Neuro-Oncology Unit, Nancy University Hospital, Nancy, France and with the Université de Lorraine, CRAN.

S. Wantz-Mézières is with the Université de Lorraine, IECL, INRIA BIGS CNRS UMR 7502, Vandoeuvre-lès-Nancy, France.

Y. Gaudeau is with the Université de Strasbourg and with the Université de Lorraine, CRAN, Vandoeuvre-lès-Nancy, France.

J.-M. Moureaux is with the Université de Lorraine, CRAN, Vandoeuvre-lès-Nancy, France.

A. Darlix is with the Department of Medical Oncology, Institut régional du Cancer de Montpellier ICM Val d'Aurelle, Montpellier, France.

N. Menjot de Champfleur and H. Duffau are with the Neuro-Oncology Unit, Montpellier University Hospital, Montpellier, France.

This article has been accepted for publication in a future issue of this journal, but has not been fully edited. Content may change prior to final publication. Citation information: DOI 10.1109/JBHI.2018.2834159, IEEE Journal of Biomedical and Health Informatics

gliomas (tumor present in different areas of the brain) [14]. For these patients, chemotherapy is prescribed in order to reduce tumor infiltration or tumor size and subsequent surgery considered [1]. Studies have shown that chemotherapy allows a decrease in tumor diameter in the majority of cases [15], in particular for patients with 1p/19q co-deletion. Chemotherapy for DLGGs can be based on the combination of Procarbazine, CCNU and Vincristine (PCV) or on Temozolomide (TMZ). TMZ chemotherapy is preferred [4], [16]–[18] because of its efficiency and its better tolerance by patients compared to PCV chemotherapy. In the case of tumor progression after rounds of chemotherapy, radiotherapy is proposed as a therapeutic option. However, because of the cognitive impairment induced by this treatment, radiation treatment indications have been reduced [14].

Provided that TMZ chemotherapy is well tolerated by the patient, the duration of this treatment is not clearly defined. In current clinical practice, an empirical case-by-case approach is adopted to address this issue. We propose to model the response of tumor diameter, the main predictor currently used to monitor patients under chemotherapy, in order to predict the time of discontinuation of chemotherapy. Our goal is to improve patients' management under chemotherapy by helping clinicians design a personalized treatment. For this work, we focus on DLGG under TMZ chemotherapy as a first-line of treatment. Indeed, in order to exclude any resistance acquired during a previous round of chemotherapy or radiotherapy, our patient population will have had no previous treatment except surgery at more than three months from the start of chemotherapy.

We are aware of other studies [19]–[21] which tackle the same problem. The models in these studies are on a cellular microscopic scale.

In [20], the authors adopt the model proposed by [19], which is a predictive model that is based on a system of partial differential equations. This model follows the evolution of tumor diameter of DLGG during a first treatment of TMZ chemotherapy and integrates molecular parameters such as 1p/19q co-deletion and IDH1 mutation. Its formulation is based on the distinction between two classes of tumor cells, proliferative cells and quiescent cells, both of which can acquire resistance to TMZ. It was tested on DLGG patients and was able to predict, after three months of chemotherapy, the minimum reached tumor size and the duration of the response up to two years after the initiation of TMZ. Nevertheless, this model is based on biological assumptions that are difficult to verify.

The second microscopic model [21] uses the hypotheses of the previous model without taking into account the resistance of proliferative cells to TMZ. Based on simulations and not on actual patient data, this predictive model attempts to minimize the number of DLGG cells at the end of TMZ chemotherapy. The simulations carried out were for short (one month) and long (30 months) treatment periods. For the duration of the short treatment, a zero value dose of TMZ was taken and the administered dose was increased till reaching the maximum tolerated dose. The simulation of this configuration showed an initial growth of proliferative cells and quiescent cells, followed by a sharp decrease in these cells and an increase in quiescent cells that are affected by chemotherapy from the beginning of treatment. This case corresponds to a realistic clinical configuration of administering the maximum dose of TMZ tolerated by the patient. For simulations of longer treatment duration, TMZ is administered in low doses over a longer period, reaching a maximum dose during the last five months of treatment. At the beginning of the simulation, the proliferative and quiescent cells continue their growth before decreasing abruptly at the end of treatment, where the quiescent cells affected by the TMZ increase. It should be noted that for this second simulation, the mathematical conditions of application of the model are verified over part of the study interval but not over the entire interval. Moreover, the explored case is difficult to apply in clinical practice. Overall, this latter model is based on numerical simulations without application on real cases and is based, as for the first microscopic model, on biological hypotheses that are difficult to verify.

It should be mentioned that we are aware of previous studies correlating MRI-defined abnormalities to oedema [22] and proposing cellular microscopic models of DLGG regrowth after radiotherapy [23]. The presence of this oedema indicates the existence of tumoral glioma cells, which strengthens our decision to adopt an MRI-based approach as we propose a novel data-driven macroscopic predictive model. Unlike microscopic models, macroscopic models rely on empirical, verifiable assumptions. Based on tumor diameters, our model is able to adapt to every new MRI dataset in order to predict the following tumor diameter. Moreover, the model is simple and quick to implement, making its clinical deployment easy.

The rest of the paper is organized as follows: In section two, the proposed mathematical models are detailed. Clinical dataset and results are presented in section three. Finally, section four provides a discussion and a conclusion.

It should be noted that part of this work has been published in the EMBC's international conference proceedings [24]. The present article relies on a larger dataset than the EMBC's work, enabling us to accurately validate our models. In addition to further detailing our methodology, in the present work we explore molecular factors in addition to tumor diameter as DLGG prognosis predictors for our models.

II. Proposed mathematical model

A. Model's algorithm

As described by [10], tumor diameter is a good predictor of the evolution of DLGGs and, without any treatment, its spontaneous progression over time is linear. In this work, we want to assist clinicians in their decision-making process to determine, with each new MRI, whether they should continue or stop TMZ chemotherapy. For each patient, we rely on MRI scans available from the onset of disease diagnosis. From FLAIR or T2 MRI exams, we recover tumor diameters obtained after manual segmentation by an expert using the OsiriX software. An example of this segmentation is provided in Fig. 1, also highlighting the macroscopic characteristic of DLGG.

This article has been accepted for publication in a future issue of this journal, but has not been fully edited. Content may change prior to final publication. Citation information: DOI 10.1109/JBHI.2018.2834159, IEEE Journal of Biomedical and Health Informatics

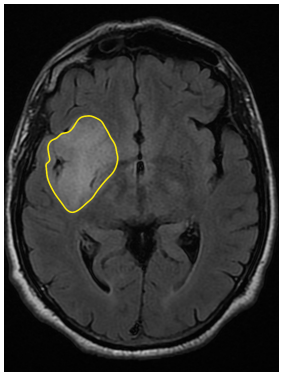

Fig. 1: FLAIR MRI slice of a Diffuse Low-Grade Glioma in the axial plane. The tumor was manually segmented (yellow) by a medical expert using OsiriX software.

For our mathematical models of tumor evolution, we are particularly interested in MRI exams during the course of the chemotherapy treatment and less than three months prior to the start of treatment. The latter time limit corresponds to the empirical period during which tumor diameter should not, according to practitioners' experience, differ considerably from the diameter after the beginning of treatment. If this information is not available, we begin the modeling at the beginning of treatment.

Tumor diameters and the time of acquisition of the MRI since the beginning of treatment represent our learning dataset. It should be noted that the number n of available data is low, often around five or six. For some validation tests in our models, we need n to be at least equal to five.
For this work, we monitored the evolution of tumor diameter under TMZ chemotherapy for a DLGGs' database. We found by observation that, for some cases, tumor diameter progression follows a linear model, while in some other cases, it follows an exponential model. But, for a few patients, tumor diameter evolution does not fit any known or specific function. One example of tumor diameter evolution over time for such patients is presented in Fig. 2.

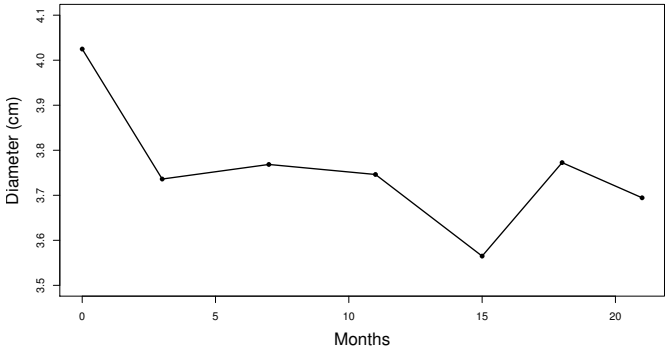

Fig. 2: An example of a tumor diameter evolution over time under chemotherapy for a patient labeled as "other".

For these patients that we label as "other", we propose a regular longitudinal follow-up of the velocity of tumor evolution under chemotherapy. If this velocity exceeds an eight mm/year threshold, showcasing a similar dynamics to that of a high-grade glioma, we alert the practitioner.
Our overall procedure is as follows: both of the linear and the exponential models are tested on each patient's set of data, and the coefficient of determination R^2 is calculated for the linear model to evaluate the quality of its prediction. In this study, if both linear and exponential models fit a patient's dataset, the corrected Akaikes Information Criterion (AICc) [25] is applied to select the best model. If neither of these models match the patient's data, we label it as an "other" case and we propose the follow-up described above.
Afterwards, we apply the selected model to predict the following tumor diameter. At the next observation, we are able to alert the clinician of any significant increase or decrease in tumor diameter, or to indicate a regular evolution that could be taken into consideration to end the treatment.
Fig. 3 summarizes the different steps of the proposed decision support algorithm. We will now describe the different models.

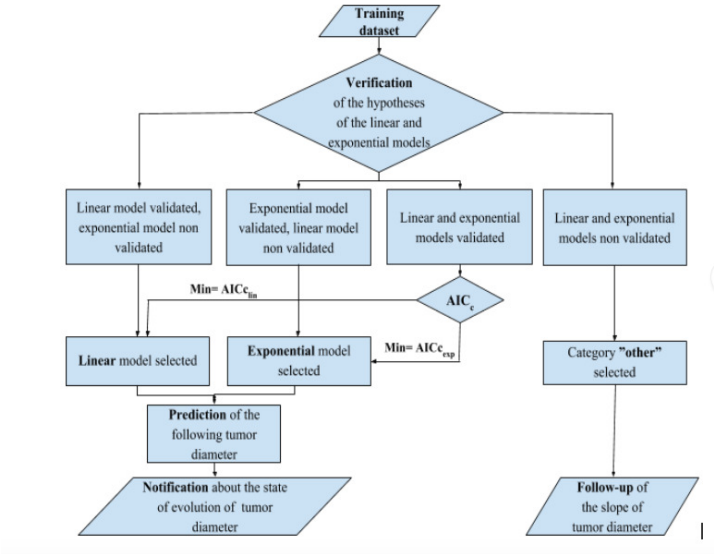

Fig. 3: Description of the proposed decision support algorithm.

B. Linear model

Let D be the random variable representing tumor diameter. This random variable follows a simple linear regression model:

$$D = b_0 + b_1 T + \epsilon \quad \text{with} \tag{2}$$

T : the random variable representing the time of observation,
ϵ : the unobserved error term.

The model's parameters are:
b_0 : the initial value of the tumor diameter,
b_1 : the growth rate of the tumor diameter.

Our prediction models rely on a training dataset $(D_i, T_i, \epsilon_i)_{i=0\ldots n}$ of size $n+1$. We assume that ϵ_i, with i

This article has been accepted for publication in a future issue of this journal, but has not been fully edited. Content may change prior to final publication. Citation information: DOI 10.1109/JBHI.2018.2834159, IEEE Journal of Biomedical and Health Informatics

being the observation number, are independent observations of a random variable following a normal distribution $\mathcal{N}(0, \sigma)$. The unknown variables are b_0, b_1 and σ. Our aim is to estimate the parameters b_0 and b_1 from the training dataset. This estimation is achieved using the least squares method which is the classical parameters' estimation method in linear regression. The details of its equations are provided in Annex A.

We start by checking the linear regression's assumptions on the training dataset. Among the hypotheses to be verified, there is the normality of the residuals ϵ_i. We choose to assess the normality hypothesis using the Shapiro-Wilk test [26] as it is relevant for a training dataset size $n \geq 5$, like in our case. It is defined as follows:

$$\begin{cases} (H_0) & \epsilon_i \text{ follows a normal distribution} \\ (H_1) & \epsilon_i \text{ does not follow a normal distribution} \end{cases} \tag{3}$$

The test statistic W is defined as:

$$W = \frac{\sum_{i=1}^{\frac{n}{2}} c_i (e_{n-i+1} - e_i)^2}{\sum_i (e_i - \bar{e})^2} \tag{4}$$

Where c_i values are derived from the Shapiro-Wilk tables and e_i is the ordered residuals' series. The hypothesis (H_0) is rejected if W_{obs}, W's realization, satisfies: $W_{obs} < W_{crit}$ (W_{crit} is supplied by the Shapiro-Wilk tables) for a given α level.

Moreover, we check the homoscedasticity condition which requires that all residuals have the same variance σ. To do this, we apply the White test [27] which is a classical test to assess the homoscedasticity for regression models. The White test is determined as follows:

$$\begin{cases} (H_0) & \sigma \text{ is constant} \\ (H_1) & \sigma \text{ is not constant} \end{cases} \tag{5}$$

The test statistic $White$ is defined as:

$$White = \frac{R^2}{1 - R^2} \frac{n-3}{2} \sim F_{2,n-3} \tag{6}$$

with
R^2 is the coefficient of determination, which is defined in Annex C.,
n is the size of the learning dataset,
$F_{u1,u2}$ is an F-distribution with parameters $u1$ and $u2$. The F-distribution is detailed in Annex D.

(H_0) is accepted if $White_{obs} < w$ (w is the quantile supplied by the F-distribution table) for a given α level.

Finally, we verify that the residuals are mutually independent by applying the Durbin-Watson test [28] which is a classical test to assess autocorrelations in regression models. It is defined as follows:

$$\begin{cases} (H_0) & \text{non-correlation of residuals} \\ (H_1) & \text{auto-correlation of residuals} \end{cases} \tag{7}$$

The test statistic DW is defined as:

$$DW = \frac{\sum_{i=1}^{n} (\epsilon_i - \epsilon_{i-1})^2}{\sum_{i=1}^{n} {\epsilon_i}^2}. \tag{8}$$

DW_{obs} value is between zero and four. If $1.5 < DW_{obs} < 2.5$, we can conclude that the residuals are not correlated. Otherwise, we deduce that there is either a positive auto-correlation ($DW_{obs} \simeq 0$), or a negative one ($DW_{obs} \simeq 4$).

After the verification of the previous hypotheses, we compute the estimated parameters $\hat{b}_0$ and $\hat{b}_1$. We then apply a t-test [29] on the $\hat{b}_1$ slope to evaluate the regression's significance. We aim here at determining whether the linear regression model adequately describes the evolution of the available datatest and at excluding the particular case of the constant linear model. The definition of this t-test is detailed in the Annex B.

We can quantify the quality of the linear model' prediction thanks to the coefficient of determination R^2. The mathematical definition of R^2 is included in Annex C. The closer R^2 values are to one, the more significant the model is for the designed dataset.

A new observation is then predicted at time T_{n+1} as follows:

$$\hat{D}_{n+1} = \hat{b}_0 + \hat{b}_1 T_{n+1}. \tag{9}$$

A prediction interval is also defined, providing the range of values in which $\hat{D}_{n+1}$ varies for a given T_{n+1}. Considering the quantiles z and for a given α level, this interval is determined as follows [30]:

$$\hat{D}_{n+1} \pm z_{\frac{\alpha}{2}, n-2} S_D \sqrt{1 + \frac{1}{n} + \frac{(T_{n+1} - \bar{T})^2}{var(T)}} \tag{10}$$

with the residual standard deviation S_D being equal to:

$$S_D = \sqrt{\frac{(D_{n+1} - \hat{D}_{n+1})^2}{n-2}}. \tag{11}$$

If the new observation D_{n+1} falls within the prediction interval, a normal evolution of tumor diameter is identified. If it leaves the prediction interval, a change in the dynamics of tumor diameter evolution is reported. This can be medically interpreted either positively (in case the diameter decreases below the lower bound of the prediction interval, presumably announcing an improved response to treatment) or negatively (tumor growth under chemotherapy over the upper limit of the prediction interval, the patient no longer responds to treatment).

This article has been accepted for publication in a future issue of this journal, but has not been fully edited. Content may change prior to final publication. Citation information: DOI 10.1109/JBHI.2018.2834159, IEEE Journal of Biomedical and Health Informatics

C. Exponential model

Let D be the random variable representing tumor diameter, following an asymptotic exponential model:

$$D = a_0 - a_1 e^{-a_2 T} + \epsilon \quad \text{with} \tag{12}$$

a_0 : the asymptotic term which ensures the data conforms to the reality that tumor diameter never equals zero, regardless of the chemotherapy's efficiency,
a_1 : the difference between the asymptotic term and the initial value of tumor diameter,
a_2 : the decay rate constant.

Our prediction models resort to a training dataset $(D_i, T_i, \epsilon_i)_{i=0...n}$ of size $n+1$. Similarly to the linear model, we assume that ϵ_i, with i being the observation number, are independent observations of a random variable following a normal distribution $\mathcal{N}(0, \sigma)$.
We start by estimating the parameters $\hat{a}_0$, $\hat{a}_1$ and $\hat{a}_2$ from the training dataset using the Gauss-Newton algorithm [31] which solves non-linear least squares regression problems. Starting from predefined initial values, a curve is generated and the sum of the squares of the learning points with respect to the curve is calculated. An estimate of the sum of the squares' variation is defined for each small change of a_0, a_1 and a_2. In the case of a nonlinear regression, the curve of the sum of the squares has an irregular shape, so that several iterations are necessary to find the optimal estimates of $\hat{a}_0$, $\hat{a}_1$ and $\hat{a}_2$ [32].
Similarly to the linear model, the normality of the ϵ_i is evaluated with the Shapiro-Wilk test.
As for the homoscedasticity condition, we plot the residuals according to the adjusted values. An inhomogeneity of the variance would be proved by an unequal distribution of the residuals along the $x = 0$ axis for the various adjusted values. The independence hypothesis is checked using the graph of each residual as a function of the preceding residual. The systematic distance of a random dispersion around the $x = 0$ axis highlights the existence of a correlation between the values of the response variable D.
After confirming these hypotheses, a t-test is applied to $\hat{a}_1$ and $\hat{a}_2$ to evaluate the significance of the regression. The details of the t-test are described in Annex B.

Once the exponential model has been validated, the diameter of a new observation is estimated as well as the prediction interval for a given α level. Depending on the position of the new observation compared to the prediction interval, reports, similar to those described for the linear model, are communicated.

D. Model selection

The choice of a prediction model depends first on the validation of the hypotheses of the linear and exponential models. If both models correspond to the patient's data, we apply the corrected Akaike information criterion $(AICc)$ which is defined as follows:

$$AIC_c = n \ln \frac{SS}{n} + 2K + \frac{2K(K+1)}{n-K-1} \tag{13}$$

with
SS : the sum of the square of the vertical distances of the points from the curve,
K : the number of parameters fitted by the regression plus one. It equals three for the linear model and four for the exponential model,
n : the size of the training dataset.

The best model is the one with the minimum value of AIC_c.

III. Clinical dataset and results

A. Clinical dataset

As part of a collaboration with Nancy and Montpellier University Hospitals, we created a DLGG database involving 55 patients who had undergone a TMZ chemotherapy as a first-line therapy. The TMZ chemotherapy was administered following a conventional regimen. This regimen included a daily dosage of 150 mg/m^2 per day for five days and, if this dosage was well tolerated, it was increased to 200 mg/m^2 per day for five days. This cycle of chemotherapy treatment was repeated every 28 days. 13 patients were excluded because they did not follow either the exponential model or the linear model. For these 13 patients, and for other similar cases, we adopt the classical approach to monitoring tumor growth dynamics: we test the slope change and if it is greater than an eight mm/year threshold (typical DLGG with a behavior similar to a high-grade glioma), we alert the practitioner with a message.
In the present article, we are particularly interested in cases of patients following either a linear or an exponential model, which represents the majority of cases in our database (42 among 55 patients). Our predictive models were therefore applied to 42 patients whose treatment lasted between nine and 32 months, with an average duration of 21.42 months. In our database, we have 24 men and 18 women with an age mean of 48.52 years. In addition, 19 among the 42 patients had known 1p/19q co-deletion and IDH1 mutation statuses. Out of these 19 patients, six are 1p/19q co-deleted with an IDH1 mutation, six are 1p/19q non-co-deleted with an IDH1 mutation and seven are 1p/19q non-co-deleted and unmutated IDH1.
It should be noted that our research was carried out following the principles of the Declaration of Helsinki.

B. Results

The average size of our training dataset is 5.523 and the α level was set at 0.1 for tumor diameter's prediction. Among the 42 patients in our database, 38 are classified as linear and four are classified as exponential. The coefficients of determination R^2 for linear patients vary between 0.73 and 0.97 with an average value of 0.89.
In Fig. 4, we showcase the prediction intervals (in green) for all 42 patients with the real diameter for linear (in red) and exponential (in blue) patients. It should be mentioned that we divided the results of the 42 patients into four different graphs in order to avoid overlaps in prediction intervals.

This article has been accepted for publication in a future issue of this journal, but has not been fully edited. Content may change prior to final publication. Citation information: DOI 10.1109/JBHI.2018.2834159, IEEE Journal of Biomedical and Health Informatics

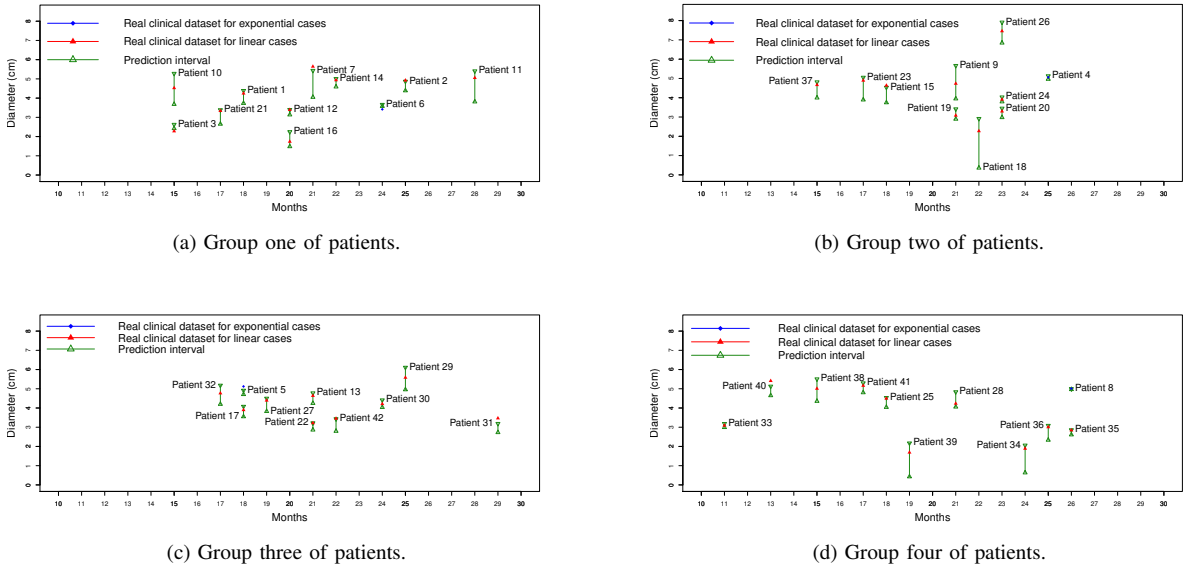

(a) Group one of patients.

(b) Group two of patients.

(c) Group three of patients.

(d) Group four of patients.

Fig. 4: Predicton intervals (green) and the real diameter for linear (red) and exponential (blue) patients.

Among the 19 patients with known 1p/19q co-deletion and IDH1 mutation statuses, we have three exponential cases and 16 linear cases. For linear patients, we have four 1p/19q co-deleted mutated IDH1 cases, five 1p/19q non-co-deleted mutated IDH1 cases and seven 1p/19q non-co-deleted unmutated IDH1 cases. As for exponential patients, we have two 1p/19q co-deleted mutated IDH1 cases and one 1p/19q non-co-deleted unmutated IDH1 case. Table I summarizes this information on the 1p/19q co-deletion and IDH1 mutation statuses for patients in our database.

In the following sections, we will present examples of each of the two predictive models. These examples generalize to the whole studied population.

1) Example for the linear model: Patient three is 1p/19q co-deleted IDH1 unmutated and underwent TMZ chemotherapy that lasted 14 months. For the training phase, we had six points that were used to predict the point preceding the end of chemotherapy.

For the linear model, the parameters $\hat{b}_0$ and $\hat{b}_1$ were estimated at 2.268 and 0.017, respectively. Furthermore, the normality hypothesis was checked with the Shapiro-Willk test: $W = 0.953 > Wcrit = 0.713$ for an α level equal to 0.01. We also validated the homoscedasticity condition with the White test: $F(2,3) = 30.82 > White = 5.0542$ for an α level equal to 0.01. Moreover, we confirmed the non-correlation hypothesis with the Durbin Watson test: $1.5 < DW = 1.9 < 2.5$. Subsequently, we verified the importance of the linear regression with a t-test on $\hat{b}_1$. We found a p-value of $0.008 \ll 0.05$ (selected α level). We also calculated the coefficient of determination R^2 which was equal to 0.85. The exponential model was evaluated as well, but since the significance of the regression was not confirmed (p-value of $\hat{a}_2 = 0.057 > \alpha = 0.05$), this model has been rejected in favor of the linear model.

Finally, we predicted the last value before the end of chemotherapy as well as the prediction interval. In Fig. 5, we visualize the training dataset as well as the predicted value.

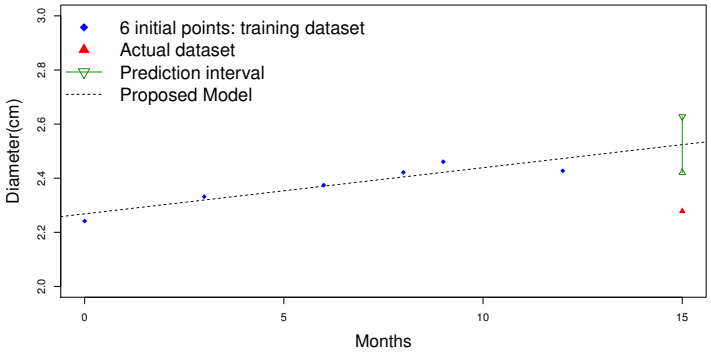

Fig. 5: Prediction of a new tumor diameter value with the linear model for patient three.

We see that the dataset follows the linear regression model and that the predicted point is below the lower bound of the prediction interval. Consequently, we indicate a significant decrease in diameter.

2) Example for the exponential model: Patient five is 1p/19q co-deleted IDH1 mutated and underwent TMZ chemotherapy that lasted 17 months.

From six training points, we were able to estimate the parameters of the exponential model $\hat{a}_0$, $\hat{a}_1$ and $\hat{a}_2$ with respective values equal to 4.80, -2.20 and 0.46. We then verified the normality hypothesis with the Shapiro-Willk test: $W = 0.959 > Wcrit = 0.713$ for an α level equal to 0.01. We also evaluated the homoscedasticity hypothesis with the graph of residuals as a function of the adjusted values (Fig. 6) and

This article has been accepted for publication in a future issue of this journal, but has not been fully edited. Content may change prior to final publication. Citation information: DOI 10.1109/JBHI.2018.2834159, IEEE Journal of Biomedical and Health Informatics

TABLE I: Distribution of the 1p/19q co-deletion and IDH1 mutation statuses in our database as well as the models corresponding to the different status classes.

Molecular status	1p/19q co-deleted IDH1 mutated	1p/19q non-co-deleted IDH1 mutated	1p/19q non-co-deleted IDH1 unmutated
Number of patients	6	5	8
Selected model	4 linear 2 exponential	5 linear 0 exponential	7 linear 1 exponential

we did not observe any particular trend of residual evolution from the adjusted values.

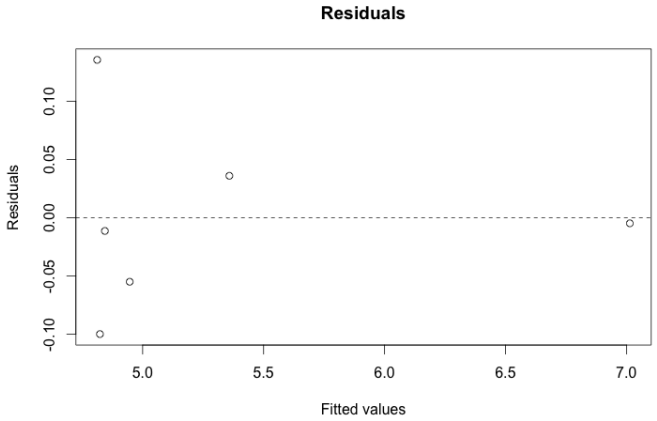

Fig. 6: Graph of residuals as a function of the adjusted values for patient five.

As for the residuals' independence hypothesis, we verified it by graphing each residual as a function of the previous residual (Fig. 7). We did not observe, in this graph, a trend of correlation between successive residuals.

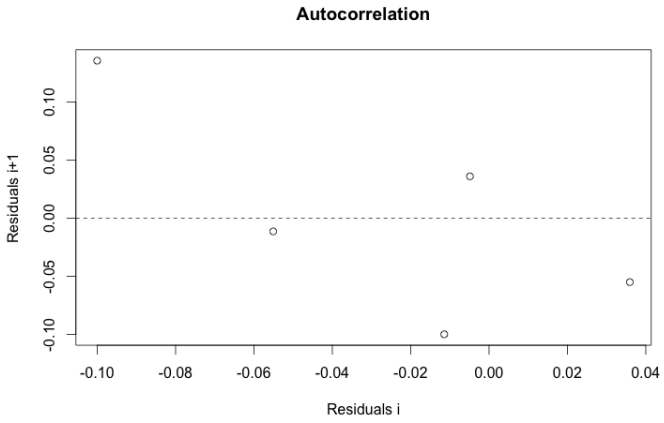

Fig. 7: Graph of each residual as a function of the previous residual for patient five.

Subsequently, we confirmed the significance of the regression by applying a t-test on $\hat{a}_1$ and $\hat{a}_2$. To do this, we compared the p-values of $\hat{a}_1$ and $\hat{a}_2$ to an α level which was set at 0.05. We found a p-value of $\hat{a}_1 = 7.28e^{-6} \ll \alpha = 0.05$ and p-value of $\hat{a}_2 = 0.01 \ll \alpha = 0.05$, leading to a significant regression.

We also tested the linear model, but as the significance of the regression was not confirmed (p-value of $\hat{b}_1 = 0.08 > \alpha = 0.05$), this model was rejected.

Using the exponential model, we finally estimated the last point before the end of the treatment as well as the prediction interval for an α level equal to 0.1. The Fig. 8 shows the curve of the training data, the predicted data, the new observation and the prediction interval. The actual data seems to fit perfectly to the exponential model and the new observation is above the prediction interval. Consequently, we indicate a significant increase in tumor diameter.

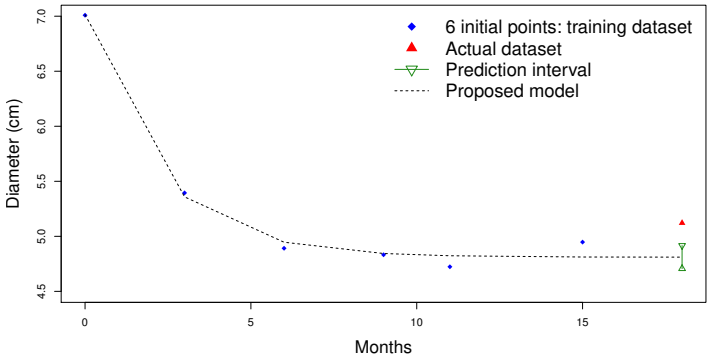

Fig. 8: Prediction of a new tumor diameter value with the exponential model for patient five.

IV. Conclusion and Discussion

In this article, we presented the different microscopic models describing the evolution of DLGG under TMZ chemotherapy. Furthermore, we proposed a new macroscopic approach to support clinicians treating DLGG patients who are undergoing a first-line TMZ chemotherapy.

Our study, conducted in partnership with Nancy and Montpellier University Hospitals, relied on a dataset from 55 patients with DLGG and who underwent TMZ chemotherapy as a first-line treatment. Based on this database, we could identify 38 patients whose disease progression fit a linear model and 4 patients whose disease progression fit an exponential model. In addition, we classified 13 patients as "other". For the "other" category of cases, we propose a regular follow-up approach using tumor dynamics' evolution under chemotherapy to detect DLGGs with a similar behavior to high-grade gliomas.

The 42 linear and exponential patients in our database had been treated from nine to 32 months, with an average duration

This article has been accepted for publication in a future issue of this journal, but has not been fully edited. Content may change prior to final publication. Citation information: DOI 10.1109/JBHI.2018.2834159, IEEE Journal of Biomedical and Health Informatics

of 21.42 months. Based on a training dataset which includes at least five MRIs, and after validating the hypotheses of the linear and exponential models, we are able to predict the following tumor diameter with great accuracy. Thanks to the corresponding prediction interval, it was possible to check whether the new observation corresponds to the predicted diameter. If the actual diameter is within the prediction range, a normal trend is notified. If not, the clinician is alerted of a significant change (increase or decrease) in tumor diameter.
It should be noted that model validation should normally be based on a different set of data from the training dataset. However, the limited number of cases did not allow this procedure to be carried out. In order to increase the size of the training dataset and to allow our models to predict the evolution of diameters during the chemotherapy period, a new protocol was set up at the Nancy University Hospital. Patients in this protocol benefit from additional non-injected MRI scans at the start of treatment. The less invasive aspect of this procedure encourages patients to participate in this protocol, enabling the learning database of the proposed models to be enhanced. Consequently, we will have a quicker access to a training dataset for each patient, allowing us to assist the clinicians more diligently than we are currently able to.
In addition, in our current database, only four out of 42 patients were classified as exponential. As we are building a larger database of DLGGs, and as we have proved that we are able to accurately predict the response of 42 patients to TMZ chemotherapy, we will be ready to propose a tailored response to the larger database, including the exponential patients. Moreover, the increase in database size would enable us to check whether or not the linear model is the prevailing model for DLGG patients undergoing a first-line TMZ treatment.
Finally, in this paper, we presented a global summary of the available 1p/19q and IDH1 encoding statuses, which are the most known molecular factors. The small number of cases with available encoding statuses (19 out of 42 patients) limits the conclusions we can draw. However, we plan to enlarge the molecular factors database thanks to more regular histological examinations and the addition of other molecular factors that significantly influence tumor growth.

APPENDIX A
EQUATIONS OF THE LEAST SQUARES METHOD FOR THE LINEAR MODEL

The estimates of b_0 and b_1 using the least squares method are defined as follows:

$$\begin{aligned} \hat{b}_1 &= \frac{cov(T,D)}{var(T)} \\ \hat{b}_0 &= \bar{D} - \hat{b}_1 \bar{T} \end{aligned} \tag{14}$$

with
$\bar{T}$ and $\bar{D}$ are the averages of T and D respectively,
$\hat{b}_0$ and $\hat{b}_1$ are the estimates of b_0 and b_1.

APPENDIX B
STUDENT TEST EQUATIONS FOR THE LINEAR AND EXPONENTIAL MODELS

The t-test on $\hat{b}_1$ for the linear model is defined as follows:

$$\begin{cases} (H_0) & \hat{b}_1 = 0 \\ (H_1) & \hat{b}_1 \neq 0 \end{cases} \tag{15}$$

(H_0) is rejected if the p-value of $\hat{b}_1$ is less than a given α level. The rejection of the null hypothesis means that the regression is significant in most cases.

The t-test, as applied to $\hat{a}_1$ and $\hat{a}_2$ is formulated as follows:

$$\begin{cases} (H_0) & \hat{a}_1 = 0 \quad \text{and} \quad \hat{a}_2 = 0 \\ (H_1) & \hat{a}_1 \neq 0 \quad \text{and} \quad \hat{a}_2 \neq 0 \end{cases} \tag{16}$$

(H_0) is rejected if the p-values of $\hat{a}_1$ and $\hat{a}_2$ are below a given α level. The rejection of the null hypothesis means that the regression is significant in most cases.

APPENDIX C
THE COEFFICIENT OF DETERMINATION

The coefficient of determination measures the fit between a linear regression model and the observed data.
Considering that $\hat{D}_i$ is the estimated diameter value at time T_i $(i = 1, ..., n)$, the coefficient of determination R^2 is defined as follows:

$$R^2 = \frac{\sum_i (\hat{D}_i - \bar{D})^2}{\sum_i (D_i - \bar{D})^2} \tag{17}$$

Its values lie between zero and one.

APPENDIX D
THE F-DISTRIBUTION

The F-distribution is a continuous statistical distribution and that is is often used to compare two variances.
If X and Y are two independent chi-square random variables with, respectively, $u1$ and $u2$ degrees of freedom, the F statistic is defined as follows:

$$F = \frac{X/u1}{Y/u2} \tag{18}$$

$F \sim F_{u1,u2}$ means that it is an F-distribution with $u1$ numerator degrees of freedom and $u2$ denominator degrees of freedom.

REFERENCES

[1] Association des Neuro-Oncologues d'Expression Française (ANOCEF), "Référentiel de l'ANOCEF pour les gliomes de l'adulte [ANOCEF reference guide for adults' gliomas]," ANOCEF, Tech. Rep., 2012.
[2] M. Baron, L. Bauchet, V. Bernier, L. Capelle, D. Fontaine, P. Gatignol, J. Guyotat, M. Leroy, E. Mandonnet, J. Pallud *et al.*, "Gliomes de grade II [Grade II gliomas]," *EMC-Neurol*, vol. 5, no. 3, pp. 1–17, 2008.

[3] D. N. Louis, A. Perry, G. Reifenberger, A. von Deimling, D. Figarella-Branger, W. K. Cavenee, H. Ohgaki, O. D. Wiestler, P. Kleihues, and D. W. Ellison, "The 2016 world health organization classification of tumors of the central nervous system: a summary," *Acta Neuropathologica*, vol. 131, no. 6, pp. 803–820, 2016. [Online]. Available: http://dx.doi.org/10.1007/s00401-016-1545-1

[4] D. Ricard, G. Kaloshi, A. Amiel-Benouaich, J. Lejeune, Y. Marie, E. Mandonnet, M. Kujas, K. Mokhtari, S. Taillibert, F. Laigle-Donadey, A. F. Carpentier, A. Omuro, L. Capelle, H. Duffau, P. Cornu, R. Guillevin, M. Sanson, K. Hoang-Xuan, and J.-Y. Delattre, "Dynamic history of low-grade gliomas before and after temozolomide treatment," *Annals of Neurology*, vol. 61, no. 5, pp. 484–490, 2007. [Online]. Available: http://dx.doi.org/10.1002/ana.21125

[5] R. B. Jenkins, H. Blair, K. V. Ballman, C. Giannini, R. M. Arusell, M. Law, H. Flynn, S. Passe, S. Felten, P. D. Brown *et al.*, "A t (1; 19)(q10; p10) mediates the combined deletions of 1p and 19q and predicts a better prognosis of patients with oligodendroglioma," *Cancer research*, vol. 66, no. 20, pp. 9852–9861, 2006.

[6] A. Idbaih, Y. Marie, G. Pierron, C. Brennetot, K. Hoang-Xuan, M. Kujas, K. Mokhtari, M. Sanson, J. Lejeune, A. Aurias *et al.*, "Two types of chromosome 1p losses with opposite significance in gliomas," *Annals of neurology*, vol. 58, no. 3, pp. 483–487, 2005.

[7] M. Sanson, Y. Marie, S. Paris, A. Idbaih, J. Laffaire, F. Ducray, S. El Hallani, B. Boisselier, K. Mokhtari, K. Hoang-Xuan *et al.*, "Isocitrate dehydrogenase 1 codon 132 mutation is an important prognostic biomarker in gliomas," *Journal of Clinical Oncology*, vol. 27, no. 25, pp. 4150–4154, 2009.

[8] E. Mandonnet, J.-Y. Delattre, M. L. Tanguy, K. R. Swanson, A. F. Carpentier, H. Duffau, P. Cornu, R. V. Effenterre, E. C. J. Alvord, and L. Capelle, "Continuous growth of mean tumor diameter in a subset of grade II gliomas," *Annals of Neurology*, vol. 53 (4), pp. 524–528, Apr. 2003.

[9] J. Pallud, D. Fontaine, H. Duffau, E. Mandonnet, N. Sanai, L. Taillandier, P. Peruzzi, R. Guillevin, L. Bauchet, V. Bernier, M. H. Baron, J. Guyotat, and L. Capelle, "Natural history of incidental world health organization grade II gliomas," *Annals of Neurology*, vol. 68 (5), pp. 727–733, Nov. 2010.

[10] E. Mandonnet, J. Pallud, O. Clatz, L. Taillandier, E. Konukoglu, H. Duffau, and L. Capelle, "Computational modeling of the WHO grade II glioma dynamics: principles and applications to management paradigm," *Neurosurgical review*, vol. 31, no. 3, pp. 263–269, 2008.

[11] J. Pallud, E. Mandonnet, H. Duffau, M. Kujas, R. Guillevin, D. Galanaud, L. Taillandier, and L. Capelle, "Prognostic value of initial magnetic resonance imaging growth rates for world health organization grade ii gliomas," *Annals of Neurology*, vol. 60, no. 3, pp. 380–383, 2006.

[12] J. Pallud, M. Blonski, E. Mandonnet, E. Audureau, D. Fontaine, N. Sanai, L. Bauchet, P. Peruzzi, M. Frenay, P. Colin *et al.*, "Velocity of tumor spontaneous expansion predicts long-term outcomes for diffuse low-grade gliomas," *Neuro-oncology*, vol. 15, no. 5, pp. 595–606, 2013.

[13] H. Duffau, "Surgery of low-grade gliomas: towards a 'functional neurooncology'," *Current opinion in oncology*, vol. 21, no. 6, pp. 543–549, 2009.

[14] L. Taillandier, "Chemotherapy for diffuse low-grade gliomas," in *Diffuse Low-Grade Gliomas in Adults*. Springer, 2013, pp. 401–422.

[15] D. Ricard, G. Kaloshi, A. Amiel-Benouaich, J. Lejeune, Y. Marie, E. Mandonnet, M. Kujas, K. Mokhtari, S. Taillibert, F. Laigle-Donadey *et al.*, "Dynamic history of low-grade gliomas before and after temozolomide treatment," *Annals of neurology*, vol. 61, no. 5, pp. 484–490, 2007.

[16] G. Kaloshi, A. Benouaich-Amiel, F. Diakite, S. Taillibert, J. Lejeune, F. Laigle-Donadey, M.-A. Renard, W. Iraqi, A. Idbaih, S. Paris *et al.*, "Temozolomide for low-grade gliomas predictive impact of 1p/19q loss on response and outcome," *Neurology*, vol. 68, no. 21, pp. 1831–1836, 2007.

[17] W. Taal, H. J. Dubbink, C. B. Zonnenberg, B. A. Zonnenberg, T. J. Postma, J. M. Gijtenbeek, W. Boogerd, F. H. Groenendijk, J. M. Kros, M. C. Kouwenhoven *et al.*, "First-line temozolomide chemotherapy in progressive low-grade astrocytomas after radiotherapy: molecular characteristics in relation to response," *Neuro-oncology*, vol. 13, no. 2, pp. 235–241, 2010.

[18] B. G. Baumert, M. E. Hegi, M. J. van den Bent, A. von Deimling, T. Gorlia, K. Hoang-Xuan, A. A. Brandes, G. Kantor, M. J. Taphoorn, M. B. Hassel *et al.*, "Temozolomide chemotherapy versus radiotherapy in high-risk low-grade glioma (eortc 22033-26033): a randomised, open-label, phase 3 intergroup study," *The Lancet Oncology*, vol. 17, no. 11, pp. 1521–1532, 2016.

[19] B. Ribba, G. Kaloshi, M. Peyre, D. Ricard, V. Calvez, M. Tod, B. Čajavec-Bernard, A. Idbaih, D. Psimaras, L. Dainese, J. Pallud, S. Cartalat-Carel, J.-Y. Delattre, J. Honnorat, E. Grenier, and F. Ducray, "A tumor growth inhibition model for low-grade glioma treated with chemotherapy or radiotherapy," *American Association for Cancer Research*, vol. 18, no. 18, pp. 5071–5080, 2012. [Online]. Available: http://clincancerres.aacrjournals.org/content/18/18/5071

[20] P. Mazzocco, C. Barthélémy, G. Kaloshi, M. Lavielle, D. Ricard, A. Idbaih, D. Psimaras, M.-A. Renard, A. Alentorn, J. Honnorat *et al.*, "Prediction of response to temozolomide in low-grade glioma patients based on tumor size dynamics and genetic characteristics," *CPT: pharmacometrics & systems pharmacology*, vol. 4, no. 12, pp. 728–737, 2015.

[21] C. Rojas, J. Belmonte-Beitia, V. M. Perez-Garcia, and H. Maurer, "Dynamics and optimal control of chemotherapy for low grade gliomas: Insights from a mathematical model." *Discrete & Continuous Dynamical Systems-Series B*, vol. 21, no. 6, 2016.

[22] C. Gerin, J. Pallud, C. Deroulers, P. Varlet, C. Oppenheim, F.-X. Roux, F. Chrétien, S. R. Thomas, B. Grammaticos, and M. Badoual, "Quantitative characterization of the imaging limits of diffuse low-grade oligodendrogliomas," *Neuro-oncology*, vol. 15, no. 10, pp. 1379–1388, 2013.

[23] M. Badoual, C. Gerin, C. Deroulers, B. Grammaticos, J.-F. Llitjos, C. Oppenheim, P. Varlet, and J. Pallud, "Oedema-based model for diffuse low-grade gliomas: application to clinical cases under radiotherapy," *Cell proliferation*, vol. 47, no. 4, pp. 369–380, 2014.

[24] M. Ben Abdallah, M. Blonski, S. Wantz-Mézières, Y. Gaudeau, L. Taillandier, and J.-M. Moureaux, "Predictive models for diffuse low-grade glioma patients under chemotherapy," in *Engineering in Medicine and Biology Society (EMBC), 2016 IEEE 38th Annual International Conference of the*. IEEE, 2016, pp. 4357–4360.

[25] G. Box, W. Hunter, and J. Hunter, *Statistics for Experimenters: an introduction to Design, Data Analysis, and Model Building*. Wiley Series in Probability and Mathematical Statistics, 1978.

[26] S. S. Shapiro and M. B. Wilk, "An analysis of variance test for normality (complete samples)," *Biometrika*, vol. 52, no. 3/4, pp. 591–611, 1965.

[27] H. White, "A heteroskedasticity-consistent covariance matrix estimator and a direct test for heteroskedasticity," *Econometrica: Journal of the Econometric Society*, pp. 817–838, 1980.

[28] J. Durbin and G. S. Watson, "Testing for serial correlation in least squares regression: I," *Biometrika*, vol. 37, no. 3/4, pp. 409–428, 1950.

[29] Student, "The probable error of a mean," *Biometrika*, pp. 1–25, 1908.

[30] D. C. Montgomery, E. A. Peck, and G. G. Vining, *Introduction to linear regression analysis*. John Wiley & Sons, 2012, vol. 821.

[31] A. Björck, *Numerical methods for least squares problems*. Siam, 1996.

[32] H. Motulsky and A. Christopoulos, *Fitting models to biological data using linear and nonlinear regression: a practical guide to curve fitting*. OUP USA, 2004.